ACS OMEGA

Open Access

http://pubs.acs.org/journal/acsodf

Article

Engineering a Fusion Protein Biomaterial Based on SpyTag/SpyCatcher Bioconjugation of Elastin and Collagen Synthetic Proteins

Pedro Toledo-Garcia, César Argüelles-Luyo, and Alberto Donayre-Torres*

Cite This: *ACS Omega* 2025, 10, 16245−16256

Read Online

ACCESS | Metrics & More | Article Recommendations | Supporting Information

ABSTRACT: Bioconjugation enables the precise control of structural and functional properties in the development of biomaterials by facilitating the covalent linkage of functional biomolecules. In this study, we developed and optimized a bioconjugation strategy to fuse recombinant proteins resembling collagen and elastin using the SpyTag/SpyCatcher system. The proteins were successfully expressed in *Escherichia coli* strain JM109(DE3) and efficiently purified via histidine affinity chromatography, attaining concentrations of 146.6 μg/mL for Scl2-ST and 124.3 μg/mL for ELP-SC. Following this, we optimized the in vitro bioconjugation process by adjusting the molar ratio of Scl2-ST to ELP-SC to 2:1, maximizing the yield of the fusion protein through the application of diafiltration. Morphological characterization of the fusion and its components was conducted using scanning electron microscopy, confirming that Scl2-ST retained its triple-helical structure, elastin-like polypeptide exhibited self-aggregation, and the fused protein formed a porous network. Our results indicate promising opportunities for scalability innovations, particularly through bioreactor-based production of the bioconjugation, which could allow for the full characterization and further development of this novel biomaterial.

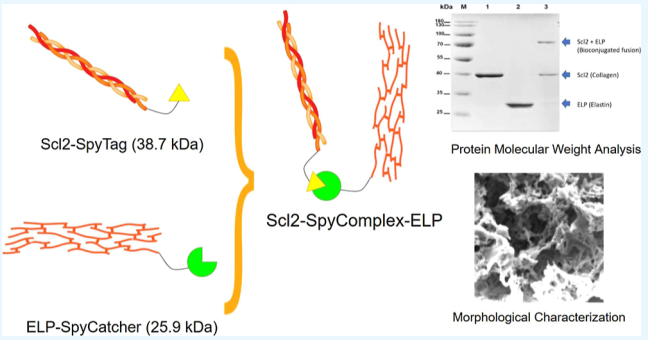

1. INTRODUCTION

Bioconjugation reaction establishes covalent bonds between at least one biomolecule and another molecule or material by chemical or biological means.[1] As bioconjugation combines the properties inherent to the starting materials,[2] it has been employed for diverse applications in the drug industry, 3D bioprinting, tissue engineering, and biomaterial innovations.[3]

Chemical conjugation via alkylation or acylation of lysine side chains has been employed in the drug industry to synthesize antibody-drug conjugates for cancer treatment.[4] Similarly, 3D bioprinting utilizes photoclick reactions, such as thiol−ene and radical-free Diels−Alder, to cross-link bioresins suitable for printing applications, even in the presence of living cells.[3,5] Tissue engineering applies the Michael-addition reaction to bioconjugate hyaluronic acid with fibrinogen, creating hydrogel scaffolds that provide mechanical and biological cues mimicking the peripheral nerve microenvironment.[6] In the field of biomaterials, the synthesis of biocompatible grafts is achieved through copper(I)-catalyzed alkyne−azide cycloaddition (CuAAC) click chemistry, enhancing drug delivery performance.[7]

These chemical conjugation methods provide materials by laborious, time-consuming, and costly procedures, requiring purified chemicals at high concentrations for polymerization-controlled reactions.[8] Therefore, efforts to simplify covalent cross-linking have been reported. A common method is the protein bioconjugation by glutaraldehyde which facilitates protein binding by interacting with lysine ε-amino and *N*-terminal groups, thereby enhancing the effectiveness of biomaterial stabilization.[9] Predominantly, collagen is cross-linked and stabilized in several protein-based materials intended for scaffold applications.[10] For instance, glutaraldehyde-cross-linking of collagen and chitosan yielded a hydrogel scaffold for adipose tissue engineering.[11] Despite its effectiveness, glutaraldehyde is highly cytotoxic and leads to calcification when exposed to cell cultures.[12,13]

Catalytic bioconjugation is a simplified approach where protein ligation is mediated by the Sortase A (SrtA) enzyme. SrtA catalyzes transpeptidation reaction from a donor peptide carrying the LPXTG motif and acceptor peptide with GGG residues.[14] This is a versatile modification method for protein labeling, bioconjugation, cross-linking, and immobilization. Synthetic tissue scaffolds of hyaluronan (HA) protein for

Received: November 13, 2024
Revised: March 21, 2025
Accepted: April 3, 2025
Published: April 16, 2025

subcutaneous implants[15] and collagen for synthetic vasculatures[16] were implemented using SrtA technology. However, enzymatic bioconjugation requires expression of the SrtA enzyme or a commercially purified product for in vitro reactions. The enzyme shows thermal and chemical stress susceptibility, somewhat limiting capabilities for novel biomaterials exploration.[17]

Bioconjugation can also be achieved by isopeptide bond formation (IBF). This is a simple spontaneous irreversible protein ligation reaction without additional components required. IBF is a natural autocatalytic bond formation found in Gram-positive bacteria and ubiquitination in human cells.[18] Adhesin members of the Cna family domain from Streptococcus pyogenes can conduct IBF.[19,20] The intramolecular bond is formed through the reaction of the ε-amino group of lysine with the side chain of asparagine or aspartate, a process catalyzed by a critical carboxyl group from glutamate or aspartate.[21]

IBF link offers multiple applications due to its strong stability under thermal, chemical, and mechanical stress.[21] Its reaction efficiency has been demonstrated under variable conditions, including temperatures of 4, 25, and 37 °C, pH ranging from 5 to 8, and the use of buffers such as PBS, phosphate-citrate, HEPES, and Tris.[20] The SpyTag (ST)-SpyCatcher (SC) peptide pair produces covalent bonds via IBF. The reaction involves a double hydrogen bond between Glu77 and Asp117, facilitating Asp117 activation. The *N*-terminus amino group of Lys31 nucleophilically attacks the *C*-terminus group of Asp117, generating a zwitterionic intermediate. This is followed by two coordinated proton transfers, where Glu77 acts as a proton shuttle. A neutral tetrahedral intermediate forms and subsequently collapses, releasing a water molecule.[22]

This reliable mechanism has been successfully used in protein fusions to create materials with unique and flexible properties.[13,22] The ST (13 a.a.) and SC (114 a.a.) peptides fused to elastin-like polypeptides (ELPs) and G proteins allowed hydrogel assembly, induced by oligomerization, useful for tissue engineering applications upon successful biocompatibility assessment.[23,24] Also, improvement in enzyme catalysis by structural cyclization is obtained when ST-SC peptides are attached to each end of the target proteins. Cyclization of β-lactamase, firefly luciferase, and xylanase increases resilience and enzyme stability.[25−27] The synthesis of silk-elastin-like polymers assembled into hydrogels mediated by ST-SC is employed for improving drug release upon combination with ELPs.[28]

Usually, protein conjugation is induced by attaching ST and SC tags to either the *N*-terminus or *C*-terminus of proteins. All components are prepurified and reactions are conducted under controlled in vitro conditions. Although the ST-SC system is highly efficient for peptide fusions, the reaction requires optimization of concentrations of each protein component to obtain the desired product.[29]

Extracellular matrix (ECM) components are desirable as novel scaffolds for tissue engineering and regenerative medicine applications. Proteins like collagen and elastin are important ECM structural components, hence recombinant expression has been evaluated.[30] The analogues Scl2 (collagen-like protein) and ELP (elastin-like protein) were produced in *Escherichia coli* and studied for mimicking ECM-like structures.[23,31−33] The design of scaffolds based on the bioconjugation of recombinant collagen and ELP proteins has yet to be studied. Therefore, it would be important to evaluate the combination of these proteins for novel tissue engineering and regenerative medicine implementations.[34]

Although *E. coli* is a suitable system for producing multiple proteins and materials, the use of ST-SC in this system has not yet been sufficiently explored and there are still few examples of methods for the expression and purification of biomaterials mediated by ST-SC.[35]

Scl2 is a bacterial collagen-like protein from S. pyogenes. Unlike human collagen, Scl2 does not undergo post-translational modification of prolines into hydroxyproline to establish the triple helical structure of collagen fibers.[36] The molecular structure of Scl2 consists of (Gly-Xaa-Yaa)n triad repeats, and it contains three primary domains: V domain at the *N*-terminus, a central collagen-like domain (CL) of 78 triplets, and an attachment domain at the *C*-terminus.[37] This protein can be engineered with structural and functional modifications to meet biomedical requirements due to its *C*-terminal modifying capabilities.[38−40] On the other hand, ELPs constitute a genetically engineered class of protein polymers derived from recurring hydrophobic motifs of human tropoelastin.[41] ELP consists of 'n' oligomeric repeats of Val-Pro-Gly-Xaa-Gly, where Xaa is any amino acid except for proline.[42] Like Scl2, ELP peptide can be attached to small molecules, fusion proteins, or site-specific conjugation reactive residues such as ST or SC for a wide variety of therapeutic applications in drug delivery and tissue repair.[43,44] No previous work has evaluated the bioconjugation of Scl2 and ELP, and therefore the morphological characteristics of the resulting biomaterial are unknown.

With Scl2 and ELP proteins as the main components of the ECM, we envision a controllable on-demand biomaterial based on molar ratio combinations of individual ECM-compatible synthetic proteins. This study holds significant potential for future approaches in tissue engineering and other biotechnological applications. Specifically, the ability to precisely combine collagen and elastin peptides through SpyTag/SpyCatcher bioconjugation technology may have multiple applications for the development of biomaterials. To this end, we explored protein expression in *E. coli*, purification, and in vitro fusion by bioconjugation of Scl2 and ELP fused to ST and SC, respectively. We report optimized conditions and a protocol for bioconjugation reactions with purified ELP and Scl2 mediated by ST-SC peptide−protein ligation. Also, preliminary biomaterial characterization by scanning electron microscopy (SEM) is reported.

2. RESULTS

2.1. Construction of Plasmids. Gene fusion sequences Scl2-ST (1140 bp) and ELP-SC (783 bp) were each cloned as *Bam*HI-XhoI fragments into the low-copy pET28a(+) vector, placing their expression under control of the T7/IPTG inducible system and adding an in-frame 6x-His tag to the resulting proteins for downstream purification. All constructs were confirmed by sequencing prior to bacterial transformation. Figure 1 shows schematics of the expression constructs used for *E. coli* expression (also see Figure S1).

2.2. Optimization of Protein Expression Conditions. We evaluated multiple conditions for increasing recombinant protein expression, as described in the experimental section. Protein yields increased 2.86 times using *E. coli* K-strain JM109(DE3) compared to the B-strain BL21(DE3), when induction was carried out using 1 mM IPTG overnight.

https://doi.org/10.1021/acsomega.4c10313
ACS Omega 2025, 10, 16245−16256

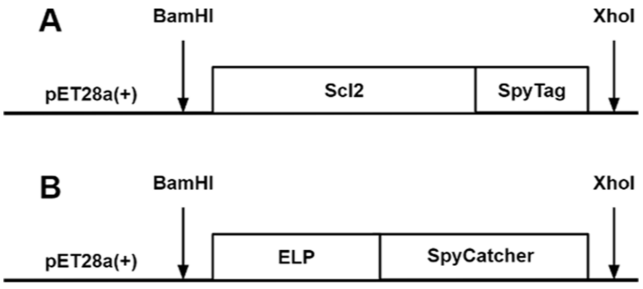

Figure 1. Schematic representations of the gene fusions Scl2-ST and ELP-SC. Both genes were cloned in the T7/IPTG inducible vector, pET-28a(+), using *Bam*HI and XhoI restriction enzymes. (A) Scl2 (collagen) fused to ST, (B) ELP (elastin-like protein) fused to SC coding sequences (see Table S1).

Cultures in Super Broth (SB) medium incubated at 37 °C produced higher accumulation of both Scl2-ST and ELP-SC recombinant proteins resulting in concentrations above 120 μg/mL compared to LB medium, which yielded 2.3 times less protein, and M9 medium in which there was no expression from the pET28a(+) plasmid. Overall, we determined that the optimal conditions for recombinant protein expression include the use of *E. coli* JM109(DE3) cells grown in SB medium, at 37 °C, with overnight induction with IPTG.

2.3. Recombinant Expression of Collagen and Elastin in *E. coli*. The expression of collagen (Scl2-ST) and elastin (ELP-SC) were evaluated by SDS-PAGE electrophoresis followed by Coomassie staining (Figure 2). As depicted, 4 h and overnight post-IPTG induction bacteria cultures show evident protein overexpression corresponding to 38.7 kDa and 25.9 kDa of Scl2-ST and ELP-SC, respectively (Figure 2, arrows). We compared total protein crude extracts from nontransformed bacteria versus IPTG-induced recombinant protein preps. The recombinant proteins were evident as protein bands of stronger intensity. We obtained higher protein levels of Scl2-ST than ELP-SC. Since, 4 h IPTG-induction produced similar yields, we decided to continue with that condition for downstream procedures.

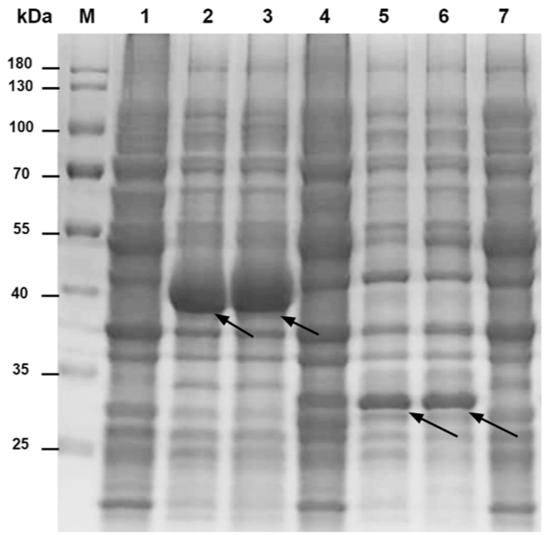

Figure 2. Scl2-ST and ELP-SC protein expression evaluation by SDS-PAGE/Coomassie staining. Protein crude extracts are used for overexpression analysis. Protein ladder (M). Lane 1, noninduced Scl2-ST protein extract. Lane 2, Scl2-ST extract (38.7 kDa) after 4 h IPTG induction. Lane 3, Scl2-ST extract after overnight IPTG induction. Lane 4 is protein extract from ELP-SC control (no IPTG). Lane 5 and 6, IPTG-induced ELP-SC (25.9 kDa) 4 h and overnight, respectively. Nontransformed *Escherichia coli* JM109(DE3) protein extract is shown in lane 7. Arrows indicate expected Scl2-ST (lanes 2 and 3) and ELP-SC (lanes 5 and 6) overexpression bands.

2.4. Protein Purification. Heterologous proteins expressed in *E. coli* K-strain JM109(DE3) were isolated following the procedure described in the experimental section. The purification was conducted using ion metal affinity chromatography (IMAC). We compared two independent IMAC methods: HisLink (Promega) and His-Gravitrap (Cytiva). The former is a quick method for processing aliquots directly from culture broth, the latter is a volume-scalable harvesting cell biomass in a multistep configuration. Following the manufacturers' recommendation, the final elution volume of purified protein from each method was 200 μL and 1.5 mL, respectively. Next, we analyzed the quality and purity of isolated proteins by SDS-PAGE and Coomassie staining (Figure 3). In each method, we obtained single isolated proteins (Figure 3, arrows) that confirmed the purity and integrity of Scl2-ST and ELP-SC proteins.

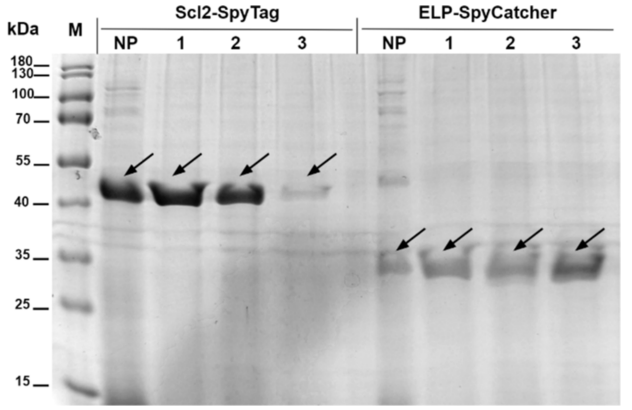

Figure 3. Comparison of two IMAC purification methods. Analysis of protein eluted fractions' purity by Coomassie staining. Protein ladder (M). Bacteria protein crude extracts or nonpurified (NP). Purification elution fraction applying the HisLink method (Lanes 1). First elution fractions of protein purification applying His-GraviTrap method (Lanes 2). Second elution fractions of protein purification applying His-GraviTrap method (Lanes 3).

The protein concentration from purified protein eluted fractions was calculated by the Bradford assay. In Table 1, we compared yields from HisLink and His-GraviTrap methods. Purified protein is reported as micrograms obtained from IMAC purification per milliliter of culture broth harvested and processed (μg/mL). His-GraviTrap resulted in similar protein yields for Scl2-ST and ELP-SC, unlike the HisLink method.

Table 1. Protein Yields Using Two Different Purification Methods

method	construct	protein concentration (μg/μL)	elution volume (μL)	yield (μg/mL)
HisLink	Scl2-ST	0.043	200	12.4
	ELP-SC	0.063	202	18.1
His GraviTrap	Scl2-ST	0.029	2938	3.4
	ELP-SC	0.040	2880	4.6

https://doi.org/10.1021/acsomega.4c10313
ACS Omega 2025, 10, 16245−16256

Overall, at least three times more protein was obtained from the quick purification assay. Nevertheless, the latter method configuration is not intended for scalable protein purification. Thus, considering our conditions and desire to scale up our system, we concluded that the most suitable method would be the His-Gravitrap, despite having a lower yield. Yields represent protein micrograms obtained per mL of culture broth (μg/mL).

Prior to conducting in vitro bioconjugation, we again purified the recombinant proteins using the His-Gravitrap method with a larger culture batch of 300 mL for each protein. Then, the purity of protein purification fractions were analyzed by SDS-PAGE/Coomassie staining. As shown in Figure 4,

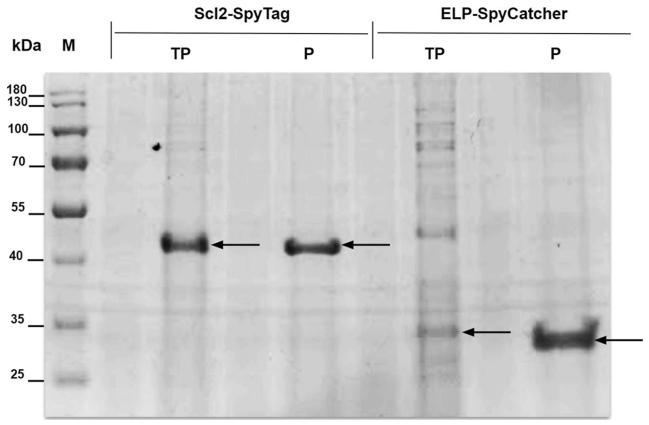

Figure 4. Coomassie-stained gel of purified Scl2-ST and ELP-SC. Analysis of purified Scl2-ST and ELP-SC proteins from 300 mL growth media using His-GraviTrap method. One microgram of protein was loaded into each lane. Protein ladder (M). Total protein samples (TP). Purified protein samples (P).

Coomassie staining analysis confirmed the presence of isolated proteins as unique bands from IMAC purification. We compared total protein extract preps (TP) versus IMAC eluted fractions (P). Expected bands of 38.7 kDa and 25.9 kDa corresponding to Scl2-ST and ELP-SC are shown from Coomassie staining (Figure 4, arrows). This result confirms that purification was performed successfully using a larger volume of culture.

Afterward, we determined the protein concentrations in the new purified eluted fractions by the Bradford assay (Table 2). Then, the molar concentration from individual proteins was calculated for setting up in vitro bioconjugation reactions.

Table 2. Protein Concentration Results from IMAC Purification

protein	concentration (μg/mL)	molar concentration (μM)	yield (μg/mL)
Scl2-ST	146.61	3.79	4.40
ELP-SC	124.27	4.80	3.73

In this purification experiment, higher concentrations (μg/mL) of Scl2-ST than ELP-SC were obtained. Despite that, the molar concentration is greater for the latter since it is a smaller protein (25.9 kDa) than Scl2-ST (38.7 kDa). In this case, yields are similar to the ones reported in Table 1.

2.5. Bioconjugation of Collagen-like and Elastin-like Proteins. Purified proteins Scl2-ST and ELP-SC were dialyzed and imidazole was removed by continuous washes using 100 mM phosphate buffer as described in the experimental section. Therefore, bioconjugation reactions were conducted in elution buffer lacking imidazole. Reactions at equimolar concentrations of 0.5 μM were incubated at room temperature for 2, 4, and 18 h. Since the ST/SC percentage of reconstitution (bioconjugation efficiency) at equimolar conditions is protein concentration-independent,[20] we also tested eluted protein fractions directly from IMAC purification (5 μM) containing imidazole to test the effect of this agent during bioconjugation reaction. Figure 5 shows reactions with and without imidazole.

As expected, the resulting fusion protein migrated between 65 and 70 kDa in both dialyzed and nondialyzed treatments as shown from Coomassie staining (Figure 5A,B). Bioconjugation reaction yielded a single fusion protein after 2, 4, and 18 h of incubation. It seems that extending the incubation time overnight (18 h) promotes greater fusion protein concentration. Using ImageJ, we quantified the band areas for each time point and compared it in terms of percentage with the bands corresponding to the unconsumed reactants (reconstitution percentage). After 18 h of incubation, a bioconjugation efficiency of 42.07% is obtained for the dialyzed treatment and 60.81% for the nondialyzed treatment compared to 17.17% (2 h)/23.33% (4 h) and 43.95% (2 h)/50.24% (4 h), for the same treatments, respectively. Nevertheless, in all reaction times tested, reactants Scl2-ST and ELP-SC were not fully consumed (Figure 5). Even when samples were incubated for up to 1 week, reactions did not run to completion (data not shown). Consequently, to optimize bioconjugation and fusion protein yields different molar ratios of Scl2-ST/ELP-SC protein were assayed, which are as follows: 0.5/2.5, 1.0/2.0, 1.5/1.5, 2.0/1.0, and 2.5/0.5 μM (Figure 6). A total of 3 μM protein was used in each reaction.

The fusion protein, combining Scl2-ST and ELP-SC, was detected in all molar ratio combinations (Figure 6). Following an 18 h overnight reaction, elastin-like and collagen-like proteins are still detected from Coomassie staining and Western blot, indicating these proteins are not fully consumed under these bioconjugation conditions. The molar ratios tested, 0.5/2.5, 1.0/2.0, 1.5/1.5, 2.0/1.0, 2.5/0.5, showed that reactant amounts influence the concentration of fusion protein obtained.

Given that the total amount of protein is the same in each reaction (3 μM), we again used ImageJ processing of Coomassie staining images to calculate the efficiency of bioconjugation, based on the percentage of nonconsumed reactants relative to the fusion protein, after 18 h reaction (Figure 7).

The efficiency of bioconjugation was calculated as the percentage of fusion protein obtained relative to nonused-up reactants (Figure 7). As depicted, in reactions containing 3 μM total of the ST and SC peptides, reactants are not fully consumed. The combination of Scl2-ST and ELP-SC in 0.5/2.5 μM ratio produced the lowest fusion protein observed (11.87%). In this reaction, the ELP-SC concentration is the highest evaluated. Conversely, the corresponding opposite mix 2.5/0.5 μM ratio, in which ELP-SC concentration is low, produced one of the greatest amounts of fusion protein (36.95%), along with the 2.0/1.0 μM ratio (37.94%). According to our results, keeping ELP-SC concentration in a low proportion favors the in vitro bioconjugation reaction. Around 3.2 times more Scl2-ELP fusion protein is yielded in this configuration (Figure 7, upper and lower quantifications). Also, equal molar concentration produces 31.89% bioconjuga-

https://doi.org/10.1021/acsomega.4c10313
ACS Omega 2025, 10, 16245−16256

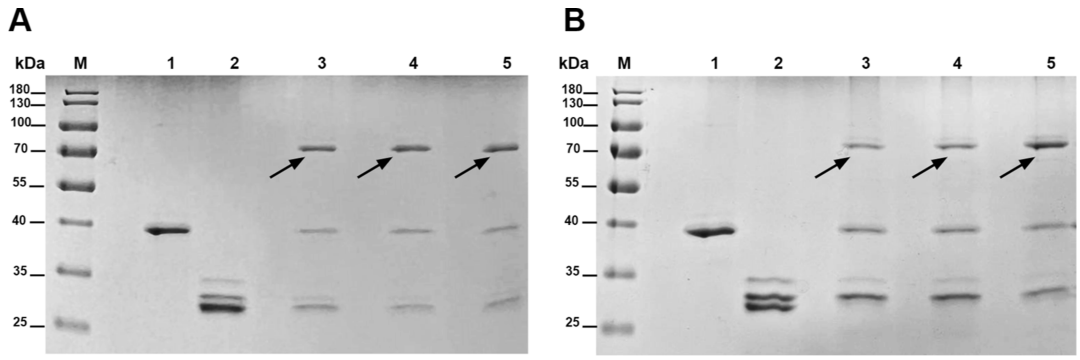

Figure 5. Effect of dialysis on protein bioconjugation. Analysis of bioconjugation reactions with nondialyzed (A) and dialyzed (B) protein preps. Scl2-ST (lanes 1) and ELP-SC (lanes 2) purified proteins after 2 h (lanes 3), 4 h (lanes 4), and 18 h (lanes 5) incubation at room temperature (arrows). Equimolar bioconjugation reactions were set up at 5 μM (A) and 0.5 μM (B). Protein ladder (M).

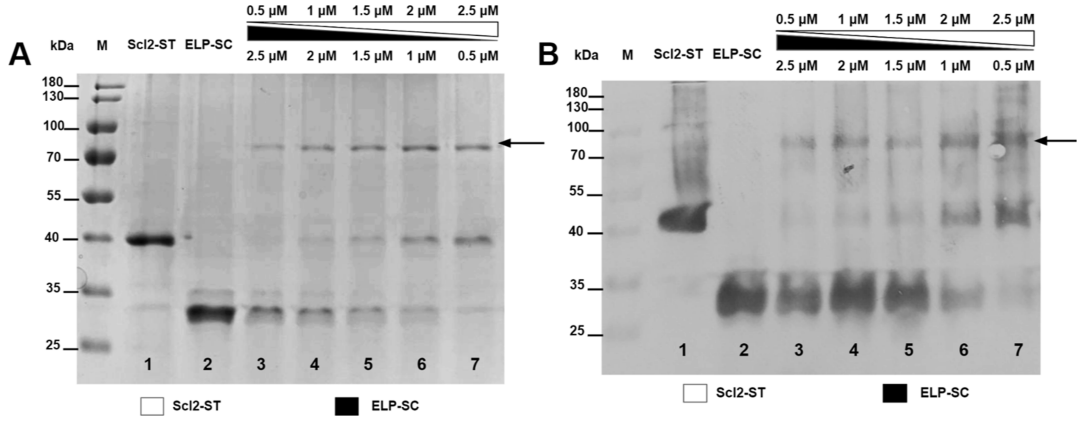

Figure 6. Analysis of Scl2-ST and ELP-SC bioconjugation under a gradient of molar concentration ratios. (A) Coomassie-stained 12% SDS-PAGE gel of protein bioconjugation at different molar ratios after overnight incubation. Protein ladder (M). Lanes 1 and 2 correspond to the proteins Scl2-ST (38.7 kDa) and ELP-SC (25.9 kDa), respectively. Lanes 3 to 7 show the evaluated molar ratios (0.5/2.5, 1.0/2.0, 1.5/1.5, 2.0/1.0, 2.5/0.5). (B) Western blot analysis with antihistidine (His) antibodies shows the presence of the bioconjugation product and reactants. Arrows show the bioconjugation fusion proteins. All reactions were conducted at room temperature.

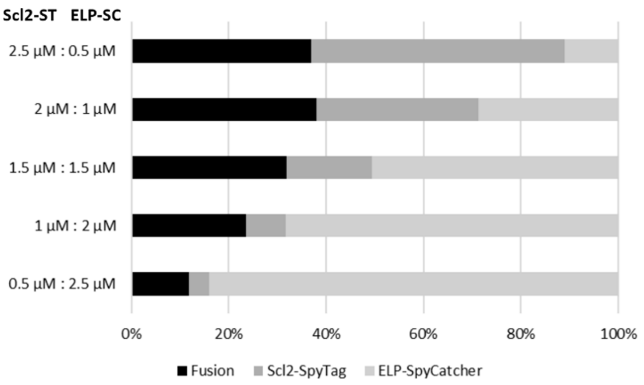

Figure 7. Estimation of bioconjugation reaction efficiency after 18 h of incubation. Scl2-ST and ELP-SC as reactants in molar concentrations. Band areas from Coomassie-stained gel were measured using ImageJ and plotted according to their proportion to the total protein. In all reactions, 3 μM of protein is used and represents 100% of the total biomass. The colored bars show the efficiency of the reaction relative to the fusion protein amounts (black regions).

tion efficiency. In summary, we evidenced that a minimal threshold in reactants is affecting efficiency. This optimal threshold starts in equimolar ratio and it is improved by decreasing the proportion of ELP-SC protein.

Subsequently, in vitro reactions were assayed with increasing protein concentrations. The optimized molar ratio of 2:1 was tested. In vitro reactions combining Scl2-ST and ELP-SC proteins at concentrations of 3.79 μM and 1.89 μM, respectively, were incubated overnight (18 h) (Table 2 and Figure 8). We expected to obtain a higher bioconjugation efficiency since reactant concentrations are increased while maintaining the optimal molar ratio.

When the total protein concentration in the bioconjugation reaction was almost doubled (from 3 to 5.7 μM), an efficiency of 49.67% was obtained (Figure 8). Thus, an increase in Scl2-ST/ELP-SC bioconjugated fusion protein is achieved compared to the previous 37.94%. This result indicates that the 2:1 molar ratio yields the best bioconjugation efficiency and that increasing reactant concentrations can also favor the reaction efficiency. However, similar to the previous assay, reactants Scl2-ST and ELP-SC are not completely consumed in the reaction. Here, we reported for the first time the efficiency of an in vitro bioconjugation for biomaterial construction using ST and SC peptides, along with testing molar ratio concentrations for establishment of reaction efficiency.

2.6. Diafiltration of Bioconjugated Protein. The in vitro reactions yielded a bioconjugated protein with Scl2 and ELP peptides linked by a covalent bond. The reaction is conducted during 18h at room temperature. As the

https://doi.org/10.1021/acsomega.4c10313
ACS Omega 2025, 10, 16245−16256

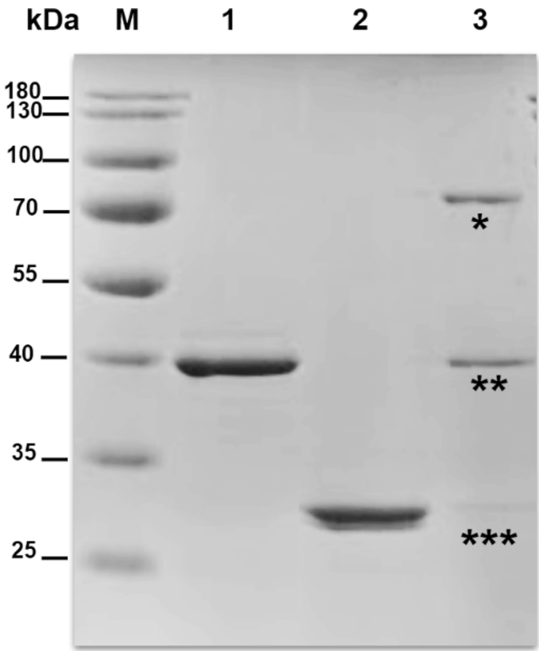

Figure 8. Bioconjugation at a molar ratio 2:1 Scl2-ST/ELP-SC. Coomassie-stained 12% SDS-PAGE gel of bioconjugation after overnight (18h) incubation. Protein ladder (M). Individual Scl2-ST protein (lane 1). Individual ELP-SC protein (lane 2). Bioconjugation reaction product (*) along with residual Scl2-ST (**), and ELP-SC (***) (lane 3). Equal volumes of 10 μL of protein were loaded in each well.

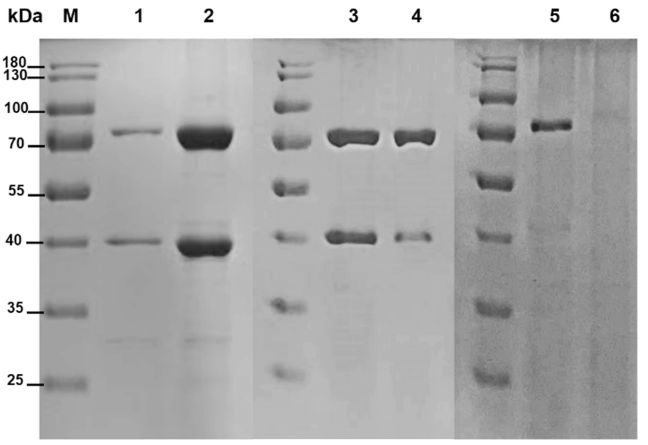

Figure 9. Diafiltration of the bioconjugated protein. Coomassie-stained 12% SDS-PAGE gel of diafiltration iterations for desalting, purifying, and concentrating the fusion protein. Protein ladder (M). Bioconjugation reaction at a molar ratio 2:1 (lane 1). Bioconjugation after diafiltration (50 kDa cutoff Amicon tube) for the first time (lanes 2 and 3). Second diafiltration in which the optimized concentration of ELP-SC was added (lane 4). Third diafiltration in which a complete and purified fusion protein was obtained (lane 5). Flow-through of the last diafiltration (lane 6). Equal volumes of 10 μL were loaded in each well.

intermediates are still present in the reaction, a diafiltration cutoff procedure through 50 kDa Amicon tubes was evaluated for separating intermediates from the 64.6 kDa fusion protein.

The in vitro reaction mix described in Figure 8 was loaded into the 50 kDa cutoff Amicon tube. Due to testing conditions, just 3 mL of the whole bioconjugation sample was used for this procedure. The diafiltration steps were conducted under the following conditions: centrifugation at 5000*g* for 30 min at 4 °C. The retained biomass was resuspended with PBS as described in the methods. This procedure allowed protein concentration and separation of intermediates. To this end, we conducted several rounds of diafiltration.

The first diafiltration completely removed the ELP-SC protein (Figure 9; lane 2), and both the fusion protein (64.6 kDa) and Scl2-ST (38.7 kDa) were retained in the Amicon filter. Noticeably, the Scl2-ST protein (below the Amicon filter molecular weight cutoff (MWCO) of 50 kDa) was also retained, likely due to low filtration efficiency because of short differences between the MWCO and the fusion MW. According to the manufacturer, to achieve the most efficiency, the MWCO should be at least 2−3 times smaller than the protein MW. Following Bradford's quantification of the total protein retained fraction (Table S2), percentages of the bands from the Coomassie-stained gel (Figure 9; lane 2) were calculated using ImageJ. Based on this quantification, the concentration of proteins observed was calculated in the retained mix collected postcentrifugation from Amicon tubes. As described in Table S2 (see Supporting Information), the concentrations of the fusion protein and Scl2-ST were 77.45 and 57.16 μg/mL, respectively. We then hypothesized that by providing ELP-SC protein to the reaction mixture at the optimized ratio (2:1), bioconjugation efficiency would increase, reducing Scl2-ST. As such, we combined 200 μL of ELP-SC at 0.74 μM with 200 μL of the mix containing 1.48 μM of Scl2-ST. Following overnight incubation of the reaction at room temperature, the sample was centrifuged for 30 min with the previously mentioned conditions. Then, the retained fraction was again assessed in a Coomassie-stained gel (Figure 9; lane 4).

The second round of diafiltration (Figure 9; lane 4) shows that Scl2-ST was largely depleted with minimal protein detected (7.45 μg/mL). Thus, a final step, following the previously mentioned procedure, was performed by adding 0.09 μM of ELP-SC protein to the mix. Following overnight incubation, a third diafiltration of the reaction yielded a single band corresponding to the intact bioconjugated fusion protein (Figure 9, lane 5).

2.7. SEM Characterization of Bioconjugated Fibers. A scanning electron microscope Inspect S50 was used to morphologically characterize the purified Scl2-ST and ELP-SC proteins, the bioconjugated fusion protein, and a sample of commercial Type I collagen (Merck, Cat no. 08-115) as a positive control (Figures 10 and 11). This analysis aimed to compare the structural features of the recombinant proteins with natural collagen and evaluate the effects of bioconjugation on the final fusion protein. Images were taken at various magnifications, allowing for both large-scale structural assessment and high-resolution surface analysis.

2.7.1. Low-Magnification Analysis. At a lower magnification (600×), the Scl2-ST sample presents an elongated fibrous structure with a diameter of approximately 15 μm and a length of 500 μm (Figure 10A). The fibers are well-defined and maintain their structure even after fixation. Similarly, Type I collagen fibers (Figure 10B), derived from mouse tails, exhibit a comparable fibrillar morphology with lengths reaching 500 μm, suggesting a structural resemblance between the recombinant and natural collagen. The maintenance of a triple-helical structure, despite glutaraldehyde fixation, further supports the structural integrity of both fiber types.

https://doi.org/10.1021/acsomega.4c10313
ACS Omega 2025, 10, 16245−16256

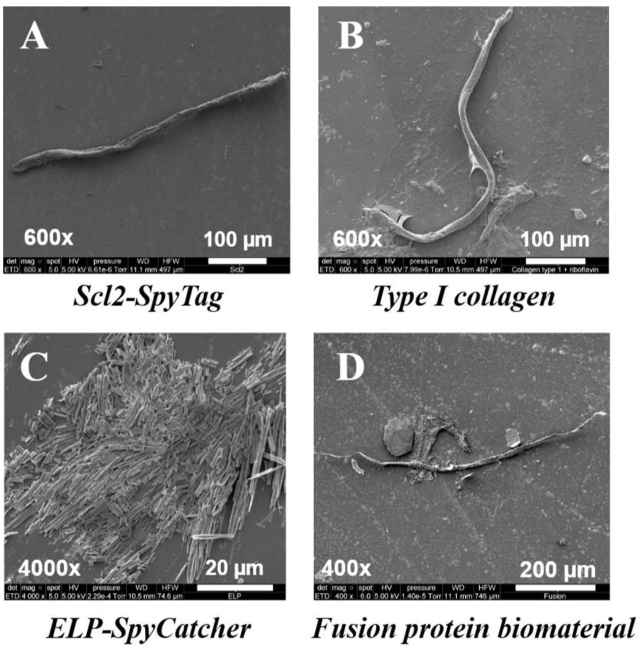

Figure 10. Morphological characterization of the fusion protein biomaterial and components. Images obtained by SEM of Scl2-ST (A), Type I collagen (B), ELP-SC (C), and fusion protein biomaterial (D) at 600×, 600×, 4000×, and 400× magnification, respectively.

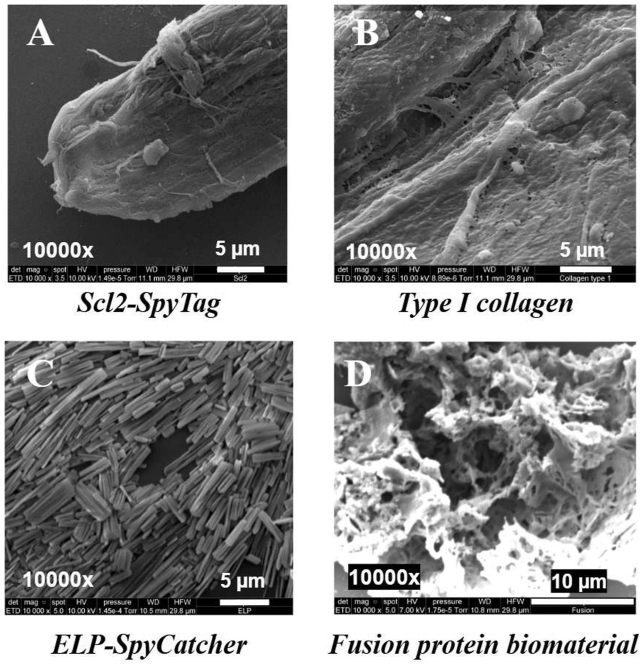

Figure 11. Morphological characterization of proteins at a higher magnification. SEM images of Scl2-ST (A), Type I collagen (B), ELP-SC (C), and fusion protein biomaterial (D) at 10,000× magnification.

The ELP-SC sample (Figure 10C) appears as an aggregation of rod-like structures but only becomes distinguishable at a higher magnification (4000×). At lower magnifications, the sample is not visible, likely due to its small tubular dimensions. This assembly phenomenon may contribute to the material's adaptability for various biomedical applications, where self-aggregation could enhance mechanical stability and functional properties.

Meanwhile, the fusion protein biomaterial (Figure 10D), at 400× magnification, exhibits a fibrous morphology along with an agglomerated structure on the left side. The fiber's length, reaching approximately 500 μm, is consistent with the lengths observed in Scl2-ST and Type I collagen (Figure 10A,B). The whole structure appears intertwined, potentially due to interactions between the Scl2-ST and ELP-SC domains during the self-assembly process. This interaction could result in enhanced mechanical properties for tissue engineering applications, offering a combination of flexibility from the elastin-like domains and structural rigidity from the collagen-like components.

2.7.2. High-Magnification Analysis. At 10,000× magnification, finer details of the protein structures become apparent (Figure 11). The Scl2-ST sample (Figure 11A) maintains its fibrillar structure, with well-defined surface characteristics that closely resemble those of Type I collagen (Figure 11B). This further reinforces the recombinant collagen's ability to mimic natural collagen at the microscale level. No significant morphological differences are observed, supporting its potential application for scaffolds.

The ELP-SC sample (Figure 11C) reveals a densely packed, tubular network with individual fibers measuring 1 μm in diameter and up to 15 μm in length. This distinct self-aggregated morphology aligns with the expected assembly behavior of ELPs, suggesting a material with tunable properties for biomedical applications.

Finally, the fusion protein biomaterial (Figure 11D) demonstrates a unique combination of fibrous and porous structures. At 10,000× magnification, the material reveals a porous matrix with pore sizes ranging from 0.5 to 1 μm, which could facilitate cell adhesion, nutrient diffusion, or other tissue engineering functions. The fibrous nature of the structure, along with the agglomerated component, indicates that the fusion of Scl2-ST and ELP-SC leads to a novel morphology that integrates key characteristics from both parent proteins. The observed porous structure, in combination with the fibrous network, could enhance the mechanical strength and biological functionality of the material, making it a promising candidate for various applications.

3. DISCUSSION

The main objective of this work was to express, purify, and assess the bioconjugation between collagen-like (Scl2-ST) and elastin-like (ELP-SC) proteins through the SpyTag/SpyCatcher system. The ST/SC system will allow future cross-linking of the recombinant proteins to obtain a scaffold-like biomaterial based on the fusion protein for tissue engineering and regenerative medicine applications.

We successfully expressed both Scl2-ST and ELP-SC in our optimized bacterial expression platform. However, a slight difference between the expressed proteins and the theoretically expected protein sizes was noticed during some gel electrophoresis analysis (Figures 3−5). We hypothesized that size discrepancy could have occurred due to sample loading problems, a distorted marker because of its position in the gel, or high salt concentration in the sample (0.07 M SDS). It has been previously reported that many proteins exhibit slightly different migration patterns when high salt concentrations are present in the buffers used to prepare proteins for electrophoresis.[45,46]

We obtained concentrations of 146.61 μg/mL for Scl2-ST and 124.27 μg/mL for ELP-SC, representing yields of 3.42 and

https://doi.org/10.1021/acsomega.4c10313
ACS Omega 2025, 10, 16245−16256

4.57 μg/mL of harvested biomass, respectively. These values are promising outcomes that align with previous studies on similar bioconjugation systems involving recombinant proteins.[47,48] Considering that both recombinant proteins were obtained from the cytoplasmic soluble phase in *E. coli*, the yields allow us to conclude that if a medium-scale bioreactor (20 L) were used, approximately 68 and 91 mg would be obtained of each protein, which are both suitable for the production of a biomaterial.[49]

The in vitro bioconjugation reaction between our precursors was successful both with and without imidazole, which demonstrates that the reaction is not affected by this chemical. Moreover, we demonstrated that the reaction is concentration-independent since it occurs at high or low protein concentrations (Figure 5). In addition, our reaction conditions, using PBS buffer, pH 7.0, incubation at room temperature, are similar to previously reported assays, where pH values varied between 6.3 and 8.3 and temperatures between 16 and 37 °C.[23,50]

Regarding bioconjugation efficiency, previous studies have demonstrated that reactant concentrations significantly impact the success rate of the reaction. Gao et al.[24] reported 100% efficiency in the synthesis of hydrogels using a globular protein GB1 fused to both ST and SC at an equimolar reactant concentration of 50 μM, without the formation of intermediates. Similarly, Zakeri et al.[20] achieved approximately 80% efficiency when bioconjugating 10 μM of equimolar Maltose Binding Protein fused to ST and SC alone. These studies utilized protein concentrations exceeding 10 μM, in contrast to the equimolar concentrations of 5 and 1.5 μM employed in our experiments, which resulted in efficiencies of 60.81% and 31.89%, respectively. These findings suggest that optimizing bioconjugation efficiency may require the evaluation of higher reactant concentrations.[20,24,51]

The position of the ST and SC tags relative to the proteins may also affect the efficiency of bioconjugation. In the designed proteins, tags positioned at the *C*-terminus ("tail") were used, resulting in an expected tail−tail fusion configuration and positioning the *N*-terminus far away from each other. This type of configuration has already been reported mainly for the bioconjugation of telechelic ELPs.[52] Although, ST and SC typically function well when fused at either the *N*-terminus or *C*-terminus,[22] in future work, a configuration in which a head−tail fusion is obtained should be explored to study its effect on bioconjugation efficiency.

To our knowledge, there is only one report examining the impact of varying molar ratios of reactants on bioconjugation efficiency using ST/SC fusion peptides. Our findings indicate that reducing the proportion of the reactant containing the SC tag and increasing the concentration of reactants, enhance bioconjugation efficiency.[51] In our experiments, Scl2-ST/ELP-SC combination at a molar ratio of 2:1 μM resulted in an efficiency of 37.94%, which further increased to 49.67% at concentrations of 3.8/1.9 μM. These results suggest that the use of equimolar concentrations, as commonly reported,[23,53] may be suboptimal at low concentrations and that decreasing the precursor containing the SC tag can improve bioconjugation efficiency. Although ELP-SC is a smaller protein by 13 kDa, we believe that this size difference is unlikely to be a significant factor in enhancing protein fusion. Instead, the enhancement may be attributed to factors such as structural docking dynamics,[54] competition, or reactant availability.

Our diafiltration experiment with Amicon tubes supports the hypothesis that reactant availability impacts bioconjugation efficiency. After concentrating the fusion protein, we continued incorporating optimal molar concentrations of the unavailable reactant into the reaction, which favored the formation of the product. We thus demonstrated that it is possible to deplete the reactants using this procedure.[55] A methodology that combines diafiltration with bioconjugation has not been previously reported. With this method, we successfully yielded a fusion protein concentration of 0.08 μM, representing nearly a 100% reaction efficiency in the final sample.

The system implemented here allows the production of biomaterials by expressing individual protein components, which then spontaneously assemble to form a fusion protein. Previous reports describe in vitro bioconjugation studies similar to the one reported here, however they use either a single protein bound to the reactive peptide or the proteins are chemically synthesized.[23,51,52] In contrast, our work used scalable production of two different proteins fused to ST/SC in a biological system, i.e., *E. coli* cells.

For potential scale-up, our implementation may provide sufficient product concentration for crystallography, circular dichroism studies, and advanced characterization of bioconjugated biomaterials.[56] Preliminarily, our morphological characterization using SEM showed that Scl2-ST exhibits a fibrous structure closely resembling type I collagen, as previously described.[57] The fibrous morphology of collagen is known to provide structural robustness, enhance mechanical properties, and promote cell adhesion,[58,59] making it a key attribute in biomaterial development.

Similarly, ELP-SC displayed a tubular structure with a diameter of approximately 1 μm, a morphology consistent with previous reports of scaffolds that support endothelial cell adhesion.[60] At 10,000× magnification, the observed tubular structures suggest that ELP-SC undergoes spontaneous aggregation, forming nano fibrillar networks similar to those reported for elastin-derived biomaterials.[61]

The bioconjugation product of Scl2-ST and ELP-SC exhibits a well-defined fibrous morphology at 400× magnification, resembling the elongated fibers observed in the Scl2-ST sample at 600×. Additionally, agglomerated regions are visible, mirroring the structural features of ELP-SC at 4000×. This structural combination provides evidence of the interaction between both proteins during bioconjugation, resulting in a hybrid morphology that integrates the characteristics of both components.

At 10,000× magnification, the fusion protein exhibits a porous structure with pore diameters between 0.5 and 1 μm. Studies suggest that pores smaller than 20 μm enhance capillarity, promoting cell diversity and facilitating migration through micropores.[62] Additionally, this porous architecture may improve cell integration, support efficient diffusion of oxygen and nutrients, and enable the controlled release of pharmaceutical agents.[63] Therefore, the fusion protein's combination of fibrous and porous morphologies could be advantageous for various tissue engineering applications.[64]

For the first time, we obtained a bioconjugated fusion protein with biomaterial characteristics using two independent proteins. By optimizing bioconjugation parameters and leveraging the ability to implement tunable combinations of collagen and elastin peptides, it is possible to yield novel textures and properties that may have widespread biomedical applications. This development facilitates the advancement of

https://doi.org/10.1021/acsomega.4c10313
ACS Omega 2025, 10, 16245−16256

new biomaterials for various applications, mainly in tissue engineering and regenerative medicine.

4. CONCLUSIONS

We demonstrated that the SpyTag/SpyCatcher bioconjugation technology enables the fusion of a collagen-like protein (Scl2-ST) and an elastin-like protein (ELP-SC), resulting in a biomaterial with potential applications in tissue engineering and regenerative medicine. By optimizing the bioconjugation reaction, we identified the optimal molar ratio (2:1 Scl2-ST/ELP-SC) to maximize reaction efficiency at low protein concentrations. Preliminary characterization using SEM confirmed that Scl2-ST retains its triple helical structure and fibrillar morphology, resembling Type I collagen, while ELP self-aggregates into a tubular network. The resulting fusion protein integrates these properties, forming a porous and fibrous matrix. Future work should focus on scaling up production and conducting further characterization to fully evaluate its potential as a biomaterial.

5. METHODS

5.1. Construction of Plasmids. We obtained ELP, Scl2, SC, and ST amino acid sequences from previous reports of *E. coli* expression (see Supporting Information).[23,65] Snapgene software was used for codon optimization for *E. coli* expression. DNA sequences codifying for ELP-SC (1140 bp) and Scl2-ST (783 bp) were synthesized and cloned into pET28a(+) plasmid by Twist Bioscience using *Bam*HI and XhoI restriction sites. DNA aliquot mixtures were transformed into *E. coli* competent cells and positive clones were selected on kanamycin plates. Plasmid DNA was expanded using a miniprep kit (Zymo Research, Cat no. D4214) and confirmed by diagnostic restriction digestion.

5.2. Optimization of Protein Expression Conditions. Bacterial strain and culturing conditions were optimized to maximize expression of Scl2-ST and ELP-SC. Biomass production and protein expression were measured in bacteria grown in Luria−Bertani (LB), M9 minimal, and SB media[66] at 30 and 37 °C. Protein yields were analyzed by SDS-PAGE stained with Coomassie blue using ImageJ quantification.[67] Two *E. coli* strains were tested, a B-strain BL21(DE3) and a K-strain JM109(DE3).[68] For comparison among culture media and bacterial strains, we assessed performance by measuring optical density (OD_{600}) at four time points during 6 h of growth. Biomass production for each treatment was evaluated considering the time to reach OD_{600} = 1. We compared cultivation periods of 7 and 18 h to determine recombinant protein accumulation postinduction.

5.3. Bacterial Transformation and Selection. *E. coli* commercial strains BL21(DE3) and JM109(DE3) were used. JM109(DE3) chemically competent cells were prepared using calcium chloride ($CaCl_2$).[69] Bacterial transformation was performed by heat shock at 42 °C for 45 s[70] Transformed cells were subsequently plated on LB/agar plates supplemented with 50 μg/mL kanamycin. Following transformation, single colonies were inoculated into 5 mL of fresh SB medium supplemented with kanamycin (50 μg/mL) for preliminary protein expression analysis.

A pilot protein expression analysis was conducted by inoculating 1/100 volumes of the preculture into fresh culture medium (5 mL) containing kanamycin (50 μg/mL).[71] Cultures were incubated with vigorous shaking at 37 °C until OD_{600} = 1. Samples were incubated for 3−4 h before induction with 1 mM IPTG. Protein accumulation was monitored over 18 h, with samples taken at 0 h (preinduction), 3, 6 h, and overnight postinduction. Recombinant protein expression was determined by Coomassie staining of SDS-PAGE gels using crude bacterial protein extracts.

Once optimal growing conditions were established, larger batches (300 mL) of broth were induced for protein purification. The bacterial biomass was harvested by centrifugation (5000*g*, 4 °C, 30 min), and the cell pellets were stored at −20 °C until protein purification.[72]

5.4. Protein Purification. We evaluated two protein purification systems, one for larger culture volumes (His GraviTrap, Cytiva, Cat no. 28401351) and another for mini preparations (HisLink, Promega, Cat no. V8823).

For purification of recombinant protein from large culture volumes, 50 mL of bacterial pellet was dissolved in 20 mL of lysis buffer (100 mM phosphate buffer, 1 M NaCl, 2 M imidazole (Cytiva, Cat no. 11-0034-00), 0.1% lysozyme (Roche, Cat no. 10837059001). Following incubation for 30 min on ice, sonication was applied in rounds of six cycles of 30 s under 50 Hz (Fisherbrand). The resulting cell lysates were cleared by 30 min centrifugation at 5000*g* and 4 °C. The supernatant was filtered using a 0.4 μM Millipore filter and directly applied to a nickel-sepharose gravity flow column (General Electric, US). Columns were pre-equilibrated with 10 mL of binding buffer (100 mM phosphate buffer, 20 mM imidazole (Cytiva)). A volume of 10 mL of binding buffer was applied to remove nonspecific protein interactions. Recombinant proteins were eluted using 3 mL of elution buffer (100 mM phosphate buffer, 500 mM imidazole (Cytiva)).[73]

For mini preparations of protein, 700 μL of bacterial culture were transferred to a microcentrifuge tube, followed by the addition of 70 μL FastBreak Reagent/DNase I solution and 75 μL of HisLink Resin. After a 30 min incubation at room temperature, the mix was transferred to a spin column, quick pulse centrifuged, and 500 μL of HisLink Binding/Wash Buffer was applied. Two rounds of washes were conducted by 5 s pulse centrifugation. The spin column was then placed in a new microcentrifuge tube and 200 μL of HisLink Elution Buffer was added. The tube was centrifuged at 19,000*g* for 1 min and the eluted protein was collected.

5.5. Protein Dialysis. Dialysis was carried out to remove imidazole from purified proteins. The total volume of eluted protein was transferred to a 14 kDa molecular weight cutoff dialysis tube (Carolina, Cat no. 684224) and immersed in 100 mM phosphate buffer (1 M Na_2HPO_4, 1 M NaH_2PO_4) overnight. This wash procedure was performed three times in total.

5.6. Protein Quantification. Concentrations of purified recombinant proteins were estimated using the Bradford Assay.[74] A standard curve was constructed from known bovine serum albumin (BSA) (Sigma-Aldrich, Cat no. A9418) protein concentrations: 0, 0.125, 0.25, 0.50, 0.75, 1.0, 1.5, and 2.0 mg/mL. Protein samples were mixed with Bradford's reagent (Merck, Cat no. B6916) at a ratio of 1:50 and incubated at room temperature for 5 min. Absorbance at 595 nm was measured in triplicate using an ELISA plate reader (Bio-Rad, Hercules, CA). Absorbance values were correlated with BSA concentrations through linear regression analysis, and the curve equation was used to calculate protein concentrations from their respective absorbance readings.

https://doi.org/10.1021/acsomega.4c10313
ACS Omega 2025, 10, 16245−16256

5.7. SDS-PAGE and Coomassie Staining. Protein expression was assessed by the detection of expected protein bands in Coomassie-stained SDS-polyacrylamide gels loaded with crude extracts. Metal affinity chromatography (IMAC) purifications were only carried out after detection of an overexpressed protein band on the gel. Typically, 2 mL of bacterial culture was processed following IPTG induction. The culture was centrifuged for 10 min at 4 °C and 4000*g*. Pellets were resuspended in 500 μL of Laemmli buffer (1X Tris/Glycine/SDS), and a 20 μL aliquot of the extract was mixed with the same volume of 2X SDS loading buffer (1 M Tris HCl pH 6.8, 10% SDS, 20% glycerol, 0.2% Bromophenol Blue). A 12% sodium dodecyl sulfate-polyacrylamide gel (SDS-PAGE) was prepared beforehand to load the samples.[73] Gels were run at 100 V for 3 h and stained with Coomassie blue (30% methanol, 10% acetic acid, 0.02% Coomassie R-250).

5.8. Bioconjugation Reactions of Scl2 and ELP. We conducted in vitro bioconjugation reactions with Scl2-ST and ELP-SC purified proteins to evaluate if varying molar ratios could improve bioconjugation efficiency. The molar concentration for each purified protein sample was calculated using the equation

$$\text{molar concentration } (\mu\text{M}) = \frac{\text{concentration } (\mu\text{g/mL})}{\text{molecular weight (kDa)}}$$

Considering the obtained molar concentrations, we assessed the molar ratios 5:1, 2:1, 1:1, 1:2, 1:5 using reactants concentrations (μM) of 2.5/0.5, 2/1, 1.5/1.5, 1/2, 0.5/2.5 Scl2-ST/ELP-SC, respectively (Table S3).

Each purified protein was diluted in PBS to the correct molar concentration for a final reaction volume of 200 μL and reaction tubes were incubated at room temperature overnight.[50] The bioconjugation efficiency of each molar ratio was determined by analyzing the expected covalent fusion on a Coomassie-stained SDS-PAGE gel. The product band pixel area was quantified using ImageJ, and the ratio of the product band area to the total bands' area in a lane was calculated.[75] Once the most efficient molar ratio was determined, bioconjugation was performed with a larger volume of reactants.

The salts, imidazole (500 mM), and residual reactants from the bioconjugation reaction were removed by a diafiltration procedure using a 50 kDa-cutoff Amicon tube (Merck, Cat No UFC905008). We aliquoted 3 mL from the bioconjugated reaction and centrifuged at 5000*g* for 30 min at 4 °C. The volume retained in the filter was resuspended with 200 μL of sterile phosphate buffered saline (1X PBS). A Coomassie-stained SDS-PAGE gel was used to assess the purity of the fusion product.

5.9. Western Blot. Recombinant proteins were analyzed by Western blot for immuno-detection. Following SDS-PAGE, proteins were transferred to a polyvinylidene fluoride (PVDF) membrane (Bio-Rad, Cat no. 1620175) at 100 V for 1 h. The membrane was treated overnight with 20 mL of blocking solution (10X TBS, 0.01% Tween-20, 5% Blocker Non-Fat Dry Milk Bio-Rad, Cat no. 1706404), followed by probing for 2 h with Mouse Anti-His Tag antibody (Bio-Rad, Cat no. MCA1396GA) diluted at 1/1000 in Tween-Tris buffered saline (TTBS). Next, the membrane was incubated for 1 h with Goat Anti-Mouse secondary antibody (Bio-Rad, Cat. no. 1706464) diluted at 1/10,000, and developed by immersion in TTBS for 30 min using an AP Color development buffer (Bio-Rad, Cat no. 1706432).

5.10. SEM. The K850 Critical Point Dryer (Quorum) was used to dry the protein samples for morphological characterization by SEM. The samples were dehydrated with ethanol and placed in the sample holder. The "K850" CPD was set at 5 °C for 4 min and then the samples were placed in the chamber. Next, liquid CO_2 was introduced into the cabinet and maintained for 3 min with stirring. Subsequently, the CO_2 and the dehydrator were slowly removed. Finally, the heater was turned on until a pressure of 1250 psi and a temperature of 35 °C were reached.

The dried samples were mounted on aluminum stubs, and gold sputtering was performed using the SPI-Module Sputter Coater (SPI Supplies). Two gold coatings of 120 s each were applied to ensure conductivity and minimize charging effects during imaging.

The morphological analysis was conducted using the Inspect S50 scanning electron microscope (FEI) at different magnifications to examine structural features across multiple scales. Low-magnification images (ranging from 400× to 600×) were used to evaluate the overall structure and organization of the protein samples. Intermediate magnifications (4000×) provided insight into self-assembly and aggregation behavior of ELP-SC. Finally, high-magnification imaging (10000×) was employed to assess fine structural details, including fiber morphology and porosity.

■ ASSOCIATED CONTENT

Supporting Information

The Supporting Information is available free of charge at https://pubs.acs.org/doi/10.1021/acsomega.4c10313.

Maps of the constructions; coding sequences of the plasmid inserts; concentrations of the samples after each diafiltration iteration; and molar concentrations for bioconjugation efficiency analysis (PDF)

■ AUTHOR INFORMATION

Corresponding Author

Alberto Donayre-Torres − *Centro de Investigación en Bioingeniería, Universidad de Ingeniería y Tecnología − UTEC, Lima 15063, Peru; Departamento de Bioingeniería e Ingeniería Química, Universidad de Ingeniería y Tecnología − UTEC, Lima 15063, Peru;* orcid.org/0000-0003-1689-8428; Email: adonayre@utec.edu.pe

Authors

Pedro Toledo-Garcia − *Centro de Investigación en Bioingeniería, Universidad de Ingeniería y Tecnología − UTEC, Lima 15063, Peru; Departamento de Bioingeniería e Ingeniería Química, Universidad de Ingeniería y Tecnología − UTEC, Lima 15063, Peru;* orcid.org/0000-0001-5978-6683

César Argüelles-Luyo − *Centro de Investigación en Bioingeniería, Universidad de Ingeniería y Tecnología − UTEC, Lima 15063, Peru; Departamento de Bioingeniería e Ingeniería Química, Universidad de Ingeniería y Tecnología − UTEC, Lima 15063, Peru;* orcid.org/0009-0003-0554-9545

Complete contact information is available at: https://pubs.acs.org/10.1021/acsomega.4c10313

Notes

The authors declare no competing financial interest.

■ ACKNOWLEDGMENTS

This research was supported by the Centro de Investigación en Bioingeniería from Universidad de Ingenieria y Tecnologia—UTEC. We thank funds provided by the Office of Research (DIN)—UTEC. The authors thank Mauricio Antunes, PhD, for his insights and for reviewing the manuscript.

■ REFERENCES

(1) Fernandes, C. S.; Teixeira, G. D.; Iranzo, O.; Roque, A. C. Engineered Protein Variants for Bioconjugation. In *Biomedical Applications of Functionalized Nanomaterials*, 2018; pp 105−138..
(2) Lavik, E.; Rotello, V. Bioconjugate Biomaterials: Leveraging Biology for the Next Generation of Active Materials. *Bioconjugate Chem.* **2022**, *33*, 543.
(3) Bednarek, C.; Schepers, U.; Thomas, F.; Bräse, S. Bioconjugation in Materials Science. *Adv. Funct. Mater.* **2024**, *34* (20), 2303613.
(4) Hafeez, U.; Parakh, S.; Gan, H. K.; Scott, A. M. Antibody−Drug Conjugates for Cancer Therapy. *Molecules* **2020**, *25* (20), 4764.
(5) Rizzo, R.; Ruetsche, D.; Liu, H.; Zenobi-Wong, M. Optimized Photoclick (Bio)Resins for Fast Volumetric Bioprinting. *Adv. Mater.* **2021**, *33* (49), 2102900.
(6) Kasper, M.; Cydis, M.; Afridi, A.; Smadi, B. M.; Li, Y.; Charlier, A.; Barnes, B. E.; Hohn, J.; Cline, M. J.; Carver, W.; Matthews, M.; Savin, D.; Rinaldi-Ramos, C. M.; Schmidt, C. E. Development of a Bioactive Tunable Hyaluronic-Protein Bioconjugate Hydrogel for Tissue Regenerative Applications. *J. Mater. Chem. B* **2023**, *11* (32), 7663−7674.
(7) Zaccaria, C. L.; Cedrati, V.; Nitti, A.; Chiesa, E.; Martinez de Ilarduya, A.; Garcia-Alvarez, M.; Meli, M.; Colombo, G.; Pasini, D. Biocompatible Graft Copolymers from Bacterial Poly(γ-Glutamic Acid) and Poly(Lactic Acid). *Polym. Chem.* **2021**, *12* (26), 3784−3793.
(8) Kalia, J.; Raines, R. Advances in Bioconjugation. *Curr. Org. Chem.* **2010**, *14* (2), 138−147.
(9) Gosling, J. P. ENZYME IMMUNOASSAY. In *Gosling199613E*, 1996; pp 287−308 .
(10) Parenteau-Bareil, R.; Gauvin, R.; Berthod, F. Collagen-Based Biomaterials for Tissue Engineering Applications. *Materials* **2010**, *3* (3), 1863−1887.
(11) Wu, X.; Black, L.; Guido, S. L.; Patrick, C. W. Preparation and Assessment of Glutaraldehyde-Crosslinked Collagen−Chitosan Hydrogels for Adipose Tissue Engineering. *J. Biomed. Mater. Res., Part A* **2006**, *81* (1), 59−65.
(12) Pal, K.; Paulson, A. T.; Rousseau, D. Biopolymers in Controlled-Release Delivery Systems. In *Modern Biopolymer Science*; Academic Press, 2009; pp 519−557..
(13) Jayachandran, B.; Parvin, T. N.; Alam, M. M.; Chanda, K.; Mm, B. Insights on Chemical Crosslinking Strategies for Proteins. *Molecules* **2022**, *27* (23), 8124.
(14) Kumari, P.; Nath, Y.; Murty, U. S.; Ravichandiran, V.; Mohan, U. Sortase a Mediated Bioconjugation of Common Epitopes Decreases Biofilm Formation in Staphylococcus Aureus. *Front. Microbiol.* **2020**, *11*, 1702.
(15) Broguiere, N.; Formica, F. A.; Barreto, G.; Zenobi-Wong, M. Sortase a as a Cross-Linking Enzyme in Tissue Engineering. *Acta Biomater.* **2018**, *77*, 182−190.
(16) Rütsche, D.; Nanni, M.; Rüdisser, S.; Biedermann, T.; Zenobi-Wong, M. Enzymatically Crosslinked Collagen as a Versatile Matrix for in Vitro and in Vivo Co-Engineering of Blood and Lymphatic Vasculature. *Adv. Mater.* **2023**, *35* (16), No. e2209476.
(17) Kiehstaller, S.; Hutchins, G. H.; Amore, A.; Gerber, A.; Ibrahim, M.; Hennig, S.; Neubacher, S.; Grossmann, T. N. Bicyclic Engineered Sortase A Performs Transpeptidation under Denaturing Conditions. *Bioconjugate Chem.* **2023**, *34*, 1114.
(18) Wani, N. A.; Stolovicki, E.; Hur, D. B.; Shai, Y. Site-Specific Isopeptide Bond Formation: A Powerful Tool for the Generation of Potent and Nontoxic Antimicrobial Peptides. *J. Med. Chem.* **2022**, *65* (6), 5085−5094.
(19) Howarth, M. Smart Superglue in Streptococci? The Proof Is in the Pulling. *J. Biol. Chem.* **2017**, *292* (21), 8998−8999.
(20) Zakeri, B.; Fierer, J. O.; Celik, E.; Chittock, E. C.; Schwarz-Linek, U.; Moy, V. T.; Howarth, M. Peptide Tag Forming a Rapid Covalent Bond to a Protein, through Engineering a Bacterial Adhesin. *Proc. Natl. Acad. Sci. U.S.A.* **2012**, *109* (12), E690−E697.
(21) Kang, H. J.; Baker, E. N. Intramolecular Isopeptide Bonds: Protein Crosslinks Built for Stress? *Trends Biochem. Sci.* **2011**, *36* (4), 229−237.
(22) Reddington, S. C.; Howarth, M. Secrets of a Covalent Interaction for Biomaterials and Biotechnology: SpyTag and SpyCatcher. *Curr. Opin. Chem. Biol.* **2015**, *29*, 94−99.
(23) Sun, F.; Zhang, W. B.; Mahdavi, A.; Arnold, F. H.; Tirrell, D. A. Synthesis of Bioactive Protein Hydrogels by Genetically Encoded SpyTag-SpyCatcher Chemistry. *Proc. Natl. Acad. Sci. U.S.A.* **2014**, *111* (31), 11269−11274.
(24) Gao, X.; Fang, J.; Xue, B.; Fu, L.; Li, H. Engineering Protein Hydrogels Using SpyCatcher-SpyTag Chemistry. *Biomacromolecules* **2016**, *17* (9), 2812−2819.
(25) Schoene, C.; Fierer, J. O.; Bennett, S. P.; Howarth, M. SpyTag/SpyCatcher Cyclization Confers Resilience to Boiling on a Mesophilic Enzyme. *Angew. Chem., Int. Ed.* **2014**, *53* (24), 6101−6104.
(26) Si, M.; Xu, Q.; Jiang, L.; Huang, H. SpyTag/SpyCatcher Cyclization Enhances the Thermostability of Firefly Luciferase. *PLoS One* **2016**, *11* (9), No. e0162318.
(27) Sun, X. B.; Cao, J. W.; Wang, J. K.; Lin, H. Z.; Gao, D. Y.; Qian, G. Y.; Park, Y. D.; Chen, Z. F.; Wang, Q. SpyTag/SpyCatcher Molecular Cyclization Confers Protein Stability and Resilience to Aggregation. *New Biotechnol.* **2019**, *49*, 28−36.
(28) Wang, S.; Huang, W.; Feng, Z.; Tian, X.; Wang, D.; Rao, L.; Tan, M.; Roongsawang, N.; Song, H.; Jiang, W.; Bai, W. Laccase-Mediated Formation of Hydrogels Based on Silk-Elastin-like Protein Polymers with Ultra-High Molecular Weight. *Int. J. Biol. Macromol.* **2023**, *231*, 123239.
(29) Keeble, A. H.; Howarth, M. Insider Information on Successful Covalent Protein Coupling with Help from SpyBank. *Methods Enzymol.* **2019**, *617*, 443−461.
(30) Mecham, R. P. Overview of Extracellular Matrix. *Curr. Protoc. Cell Biol.* **2012**, *57* (1), 10.1.1−10.1.16.
(31) Zhu, D.; Wang, H.; Trinh, P.; Heilshorn, S. C.; Yang, F. Elastin-like Protein-Hyaluronic Acid (ELP-HA) Hydrogels with Decoupled Mechanical and Biochemical Cues for Cartilage Regeneration. *Biomaterials* **2017**, *127*, 132−140.
(32) Peng, Y. Y.; Yoshizumi, A.; Danon, S. J.; Glattauer, V.; Prokopenko, O.; Mirochnitchenko, O.; Yu, Z.; Inouye, M.; Werkmeister, J. A.; Brodsky, B.; Ramshaw, J. A. M. A Streptococcus Pyogenes Derived Collagen-like Protein as a Non-Cytotoxic and Non-Immunogenic Cross-Linkable Biomaterial. *Biomaterials* **2010**, *31* (10), 2755−2761.
(33) Cosgriff-Hernandez, E.; Hahn, M. S.; Russell, B.; Wilems, T.; Munoz-Pinto, D.; Browning, M. B.; Rivera, J.; Höök, M. Bioactive Hydrogels Based on Designer Collagens. *Acta Biomater.* **2010**, *6* (10), 3969−3977.
(34) Vilaça-Faria, H.; Noro, J.; Reis, R. L.; Pirraco, R. P. Extracellular Matrix-Derived Materials for Tissue Engineering and Regenerative Medicine: A Journey from Isolation to Characterization and Application. *Bioactive Mater.* **2024**, *34*, 494−519.
(35) Keeble, A. H.; Howarth, M. Power to the Protein: Enhancing and Combining Activities Using the Spy Toolbox. *Chem. Sci.* **2020**, *11* (28), 7281−7291.
(36) Xu, Y.; Keene, D. R.; Bujnicki, J. M.; Höök, M.; Lukomski, S. Streptococcal Scl1 and Scl2 Proteins Form Collagen-like Triple Helices. *J. Biol. Chem.* **2002**, *277* (30), 27312−27318.

https://doi.org/10.1021/acsomega.4c10313
ACS Omega 2025, 10, 16245−16256

(37) Lukomski, S.; Bachert, B. A.; Squeglia, F.; Berisio, R. Collagen-like Proteins of Pathogenic Streptococci. *Mol. Microbiol.* **2017**, *103* (6), 919−930.
(38) Picker, J.; Lan, Z.; Arora, S.; Green, M.; Hahn, M.; Cosgriff-Hernandez, E.; Hook, M. Prokaryotic Collagen-like Proteins as Novel Biomaterials. *Front. Bioeng. Biotechnol.* **2022**, *10*, 840939.
(39) Qiu, Y.; Zhai, C.; Chen, L.; Liu, X.; Yeo, J. Current Insights on the Diverse Structures and Functions in Bacterial Collagen-like Proteins. *ACS Biomater. Sci. Eng.* **2023**, *9*, 3778.
(40) Humtsoe, J. O.; Kim, J. K.; Xu, Y.; Keene, D. R.; Höök, M.; Lukomski, S.; Wary, K. K. A Streptococcal Collagen-like Protein Interacts with the $\alpha 2\beta 1$ Integrin and Induces Intracellular Signaling. *J. Biol. Chem.* **2005**, *280* (14), 13848−13857.
(41) Despanie, J.; Dhandhukia, J. P.; Hamm-Alvarez, S. F.; MacKay, J. A. Elastin-like Polypeptides: Therapeutic Applications for an Emerging Class of Nanomedicines. *J. Controlled Release* **2016**, *240*, 93−108.
(42) Meyer, D. E.; Chilkoti, A. Purification of Recombinant Proteins by Fusion with Thermally-Responsive Polypeptides. *Nat. Biotechnol.* **1999**, *17* (11), 1112−1115.
(43) Bidwell, G. L. Novel Protein Therapeutics Created Using the Elastin-like Polypeptide Platform. *Physiology* **2021**, *36*, 367.
(44) Guo, Y.; Liu, S.; Jing, D.; Liu, N.; Luo, X. The Construction of Elastin-like Polypeptides and Their Applications in Drug Delivery System and Tissue Repair. *J. Nanobiotechnol.* **2023**, *21* (1), 418.
(45) Silva, R. L., Kaur, A., Gomes, A. V. Incorrect Molecular Weights due to Inaccurate Prestained Protein Molecular Weight Markers That Are Used for Gel Electrophoresis and Western Blotting. **2020**, bioRxiv (Cold Spring Harbor Laboratory)
(46) Guan, Y.; Zhu, Q.; Huang, D.; Zhao, S.; Jan Lo, L.; Peng, J. An equation to estimate the difference between theoretically predicted and SDS PAGE-displayed molecular weights for an acidic peptide. *Sci. Rep.* **2015**, *5*, 13370.
(47) Essert, A.; Castiglione, K. Dimer Stabilization by SpyTag/SpyCatcher Coupling of the Reductase Domains of a Chimeric P450 BM3Monooxygenase from *Bacillus* Spp. Improves Its Stability, Activity, and Purification. *ChemBioChem* **2024**, *25* (3), No. e202300650.
(48) Alam, M. K.; El-Sayed, A.; Barreto, K.; Bernhard, W.; Fonge, H.; Geyer, C. R. Site-Specific Fluorescent Labeling of Antibodies and Diabodies Using SpyTag/SpyCatcher System for in Vivo Optical Imaging. *Mol. Imaging Biol.* **2018**, *21* (1), 54−66.
(49) Choi, Y. J.; Bourque, D.; Morel, L.; Groleau, D.; Míguez, C. B. Multicopy Integration and Expression of Heterologous Genes in Methylobacterium Extorquens ATCC 55366. *Appl. Environ. Microbiol.* **2006**, *72* (1), 753−759.
(50) Yang, X.; Wei, J.; Wang, Y.; Yang, C.; Zhao, S.; Li, C.; Dong, Y.; Bai, K.; Li, Y.; Teng, H.; et al. A Genetically Encoded Protein Polymer for Uranyl Binding and Extraction Based on the SpyTag−SpyCatcher Chemistry. *ACS Synth. Biol.* **2018**, *7* (10), 2331−2339.
(51) Jia, L.; Minamihata, K.; Ichinose, H.; Tsumoto, K.; Kamiya, N. Polymeric SpyCatcher Scaffold Enables Bioconjugation in a Ratio-Controllable Manner. *Biotechnol. J.* **2017**, *12* (12), 1700195.
(52) Zhang, W.-B.; Sun, F.; Tirrell, D. A.; Arnold, F. H. Controlling Macromolecular Topology with Genetically Encoded SpyTag−SpyCatcher Chemistry. *J. Am. Chem. Soc.* **2013**, *135* (37), 13988−13997.
(53) Massa, S.; Devoogdt, N. *Bioconjugation Methods and Protocols*; Springer New York: New York, NY, 2019.
(54) Li, L.; Fierer, J. O.; Rapoport, T. A.; Howarth, M. Structural Analysis and Optimization of the Covalent Association between SpyCatcher and a Peptide Tag. *J. Mol. Biol.* **2014**, *426* (2), 309−317.
(55) Alele, N.; Ulbricht, M. Membrane-Based Purification of Proteins from Nanoparticle Dispersions: Influences of Membrane Type and Ultrafiltration Conditions. *Sep. Purif. Technol.* **2016**, *158*, 171−182.
(56) Prasad, R. D.; Prasad, R. S.; Prasad, R. B.; Prasad, S. R.; Singha, S. B.; Singha, A. D.; Prasad, R. J.; Sinha, P.; Saxena, S.; Vaidya, A. K.; Teli, S. B.; Saxena, U. R.; Harale, A.; Deshmukh, M. B.; Padvi, M. N.; Navathe, G. J. A Review on Modern Characterization Techniques for Analysis of Nanomaterials and Biomaterials. *ES Energy Environ.* **2024**, *23*, 1087.
(57) Panwar, P.; Du, X.; Sharma, V.; Lamour, G.; Castro, M.; Li, H.; Brömme, D. Effects of Cysteine Proteases on the Structural and Mechanical Properties of Collagen Fibers. *J. Biol. Chem.* **2013**, *288* (8), 5940−5950.
(58) Carcamo, A. S.; Goldman, M. P. Skin Resurfacing with Ablative Lasers. In *Cutaneous and Cosmetic Laser Surgery*, 2006; pp 183−247..
(59) Sancho, A.; Taskin, M. B.; Wistlich, L.; Stahlhut, P.; Wittmann, K.; Rossi, A.; Groll, J. Cell Adhesion Assessment Reveals a Higher Force per Contact Area on Fibrous Structures Compared to Flat Substrates. *ACS Biomater. Sci. Eng.* **2022**, *8* (2), 649−658.
(60) McKenna, K. A.; Hinds, M. T.; Sarao, R. C.; Wu, P. C.; Maslen, C. L.; Glanville, R. W.; Babcock, D.; Gregory, K. W. Mechanical Property Characterization of Electrospun Recombinant Human Tropoelastin for Vascular Graft Biomaterials. *Acta Biomater.* **2012**, *8* (1), 225−233.
(61) Geng, Z.; Laakko, T.; Hokkanen, A.; Södergård, C.; Maasilta, I.; Mohammadi, P. Material Engineering and Application of Hybrid Biomimetic-de Novo Designed Elastin-like Polypeptides. *Commun. Mater.* **2024**, *5* (1), 1−11.
(62) Yadav, P.; Beniwal, G.; Saxena, K. K. A Review on Pore and Porosity in Tissue Engineering. *Mater. Today: Proc.* **2021**, *44*, 2623−2628.
(63) Hernandez, J. L.; Woodrow, K. A. Medical Applications of Porous Biomaterials: Features of Porosity and Tissue-Specific Implications for Biocompatibility. *Adv. Healthcare Mater.* **2022**, *11* (9), 2102087.
(64) Heydarkhan-Hagvall, S.; Schenke-Layland, K.; Dhanasopon, A. P.; Rofail, F.; Smith, H.; Wu, B. M.; Shemin, R.; Beygui, R. E.; MacLellan, W. R. Three-Dimensional Electrospun ECM-Based Hybrid Scaffolds for Cardiovascular Tissue Engineering. *Biomaterials* **2008**, *29* (19), 2907−2914.
(65) Rahman, I.; Fang, L.; Wei, Z.; Zheng, X.; Jiazhang, L.; Huang, L.; Xu, Z. Highly efficient soluble expression and purification of recombinant human basic fibroblast growth factor (hbFGF) by fusion with a new collagen-like protein (Scl2) in Escherichia coli. *Prep. Biochem. Biotechnol.* **2020**, *50* (6), 598−606.
(66) Noor, R.; Islam, Z.; Munshi, S. K.; Rahman, F. Influence of Temperature on Escherichia coli Growth in Different Culture Media. *J. Pure Appl. Microbiol.* **2013**, *7* (2), 899−904.
(67) Rehbein, P.; Schwalbe, H. Integrated Protocol for Reliable and Fast Quantification and Documentation of Electrophoresis Gels. *Protein Expression Purif.* **2015**, *110*, 1−6.
(68) Ukkonen, K.; Veijola, J.; Vasala, A.; Neubauer, P. Effect of Culture Medium, Host Strain and Oxygen Transfer on Recombinant Fab Antibody Fragment Yield and Leakage to Medium in Shaken E. Coli Cultures. *Microb. Cell Fact.* **2013**, *12* (1), 73.
(69) Sambrook, J.; Russell, D. W. Preparation and Transformation of Competent E. coli Using Calcium Chloride. *Cold Spring Harb. Protoc.* **2006**, *2006*, pdb.prot3932.
(70) Froger, A.; Hall, J. E. Transformation of Plasmid DNA into E. Coli Using the Heat Shock Method. *J. Vis. Exp.* **2007**, 253.
(71) Elbing, K. L.; Brent, R. Growth of *E. Coli* in Liquid Medium. *Curr. Protoc. Mol. Biol.* **2019**, *125* (1), No. e81.
(72) Rad-Malekshahi, M.; Flement, M.; Hennink, W. E.; Mastrobattista, E. Optimization of the Recombinant Production and Purification of a Self-Assembling Peptide in Escherichia Coli. *Microb. Cell Fact.* **2014**, *13* (1), 178.
(73) Donayre-Torres, A. J.; Esquivel-Soto, E.; Gutiérrez-Xicoténcatl, M. d.; Esquivel-Guadarrama, F. R.; Gómez-Lim, M. A. Production and Purification of Immunologically Active Core Protein P24 from HIV-1 Fused to Ricin Toxin B Subunit in E. Coli. *Virol. J.* **2009**, *6* (1), 17.
(74) Kruger, N. J. *The Bradford Method for Protein Quantitation*; Springer Protocols Handbooks, 2009; pp 17−24..
(75) Ohgane, K.; Yoshioka, H. *Quantification of Gel Bands by an Image J Macro, Band/Peak Quantification Tool*; protocols.io, 2019.

https://doi.org/10.1021/acsomega.4c10313
ACS Omega 2025, 10, 16245−16256